6ICEGE 6th International Conference on Earthquake Geotechnical Engineering
1-4 November 2015
Christchurch. New Zealand

Unloading-Reloading Rule for Nonlinear Site Response Analysis

S. Yniesta[1], S. J. Brandenberg[2]

ABSTRACT

This paper presents a loading unloading rule for a one dimensional nonlinear stress-strain model capable of reproducing any modulus reduction and damping curve. Unlike many previous nonlinear models, the proposed model does not utilize Masing's rules, nor does it require a specific functional form such as a hyperbola. Rather, the model utilizes a coordinate transformation technique in which one axis lies along the secant shear modulus line for a particular strain level with the other axis in the orthogonal direction. Damping is very easily controlled in the transformed coordinate space. An inverse transformation returns the desired stress for any increment of strain, and the model converges independently of the amplitude of the strain increment. Small-strain hysteretic damping can also be achieved using the proposed model.

Introduction

This paper presents a new unloading and reloading rule that completely departs from Masing's rules to provide a perfect fit of a modulus reduction and damping curve. Masing's rules are a poor way to match the damping behavior of a soil because they over predict damping at large strains, and do not provide hysteretic damping at small strains. To introduce small strain damping nonlinear codes typically use frequency dependent Rayleigh damping (Rayleigh and Lindsay 1945). Rayleigh damping is typically configured to match the desired small strain damping ratio at one or two target frequencies. Several solutions have been proposed to better match damping at large strains. Darendeli (2001) created a damping reduction factor to change the shape of the unloading curve. Based on Darendeli's work, Phillips and Hashash (2009) introduced a new damping reduction factor that provides a better fit for the curve at large strains. Phillips and Hashash also introduced a full Rayleigh damping formulation that is frequency-independent. This formulation is computationally demanding. Although their model is an important achievement it does not provide a perfect fit of the damping curve. It also uses a hyperbolic fit of the modulus reduction curve, which is unable to match any target curve. The hyperbolic fit typically introduces bias at large strains rendering the models unable to capture the shear strength of the soil. Hashash et al. (2010) presented a procedure to match the strength with their model. This procedure provides a more realistic shear strength but is still imperfect. Some of the most advanced models follow the framework of plasticity, and use bounding surface algorithms (e.g. Wang et al. 1990). Although they tend to match the strength pretty well, they also over predict damping at large strains.

[1]Ph.D. Candidate, Department of Civil and Environmental Engineering, University of California, Los Angeles (UCLA), U.S.A. samuel.yniesta@ucla.edu
[2]Associate Professor, Department of Civil and Environmental Engineering, University of California, Los Angeles (UCLA), U.S.A. sjbrandenberg@ucla.edu

The new model presented in this paper departs from Masing's framework, and utilizes a coordinate transformation from the shear stress (τ) – shear strain (γ) space to the modified shear stress (τ') – shear strain (γ') space, where γ' lies in a direction parallel to the secant modulus and τ' is in the orthogonal direction. The shear stress is directly calculated from the shear strain through an inverse coordinate transformation. During initial loading the new model follows the backbone curve and keeps track of the maximum shear strain $\gamma_{in_{max}}$. The model uses a spline fitting method to create a backbone curve from a modulus reduction curve.

Mathematical Framework of the Unloading Reloading Rule

Coordinate Transformation

The mathematical transformation used by the new rule consists of a rotation of the axis by an angle θ and a translation of the frame of reference by (γ_0, τ_0). The system is rotated so the previous reversal point and the target reversal point lie on the new horizontal axis, γ'. The reference point is also translated so the center of the new coordinate system is in the middle of the previous reversal point and the target reversal point. In Figure 1, the subscript L (opposite direction of the strain increment) designates the previous reversal point, and the subscript R (same direction of the strain increment) designates the target reversal point. The target reversal stress-strain point is defined as the previous reversal point if the current reversal point is not the maximum reversal stress-strain point. Otherwise the target reversal point is defined as the opposite of the maximum reversal point, and the reference point is not translated as shown in Figure 1(a). (γ, τ) designates the original coordinate system, and (γ', τ') designates the new coordinate system.

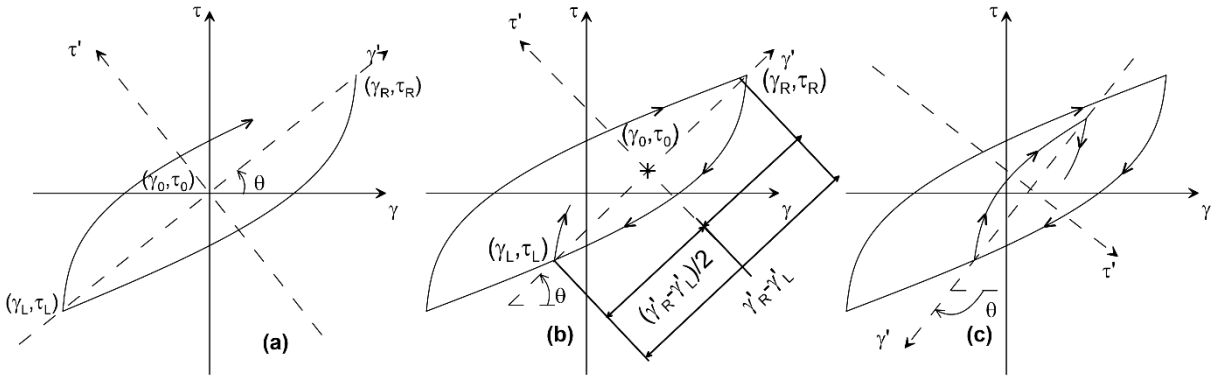

Figure 1. Stress-Strain loops during (a) Reloading; (b) Asymmetrical loading; (c) Unloading

The definition of the angle of rotation depends on the direction of loading. If the soil is being reloaded, i.e. the direction of loading is positive on γ, as shown in Figures 1(a) and 1(b), then the angle of rotation is defined by the Equation 1(a). If the soil is being unloaded, i.e. the direction of loading is negative (Figure 1(c)), and the angle of rotation is defined by the Equation 1(b).

$$\theta = \tan^{-1}\frac{\tau_R - \tau_L}{\gamma_R - \gamma_L} \tag{1a}$$

$$\theta = \pi + \tan^{-1}\frac{\tau_R - \tau_L}{\gamma_R - \gamma_L} \tag{1b}$$

The point of reference is translated from (0,0) to (γ_0, τ_0) . The new point of reference has the following coordinates in the initial axis system:

$$\gamma_0 = \frac{\gamma_R + \gamma_L}{2} \tag{2}$$

$$\tau_0 = \frac{\tau_R + \tau_L}{2} \tag{3}$$

The coordinates in each system can be expressed in terms of the coordinates in the other system:

$$\begin{pmatrix}\gamma \\ \tau\end{pmatrix} = \begin{pmatrix}\gamma' \cos\theta - \tau' \sin\theta + \gamma_0 \\ \gamma' \sin\theta + \tau' \cos\theta + \tau_0\end{pmatrix} \tag{4}$$

$$\begin{pmatrix}\gamma' \\ \tau'\end{pmatrix} = \begin{pmatrix}(\gamma - \gamma_0)\cos\theta + (\tau - \tau_0)\sin\theta \\ -(\gamma - \gamma_0)\sin\theta + (\tau - \tau_0)\cos\theta\end{pmatrix} \tag{5}$$

Calculation of the New Stress

Once the mathematical transformation is algebraically defined, a function can be chosen to describe the stress-strain relationship. In the transformed system we use a biquadratic equation to describe the stress:

$$\tau' = a\,\gamma'^4 + b\,\gamma'^2 + c \tag{6}$$

With *a*, *b*, and *c* coefficients defined by three conditions to control the shape of stress-strain loop (Equations 8-10). This function was selected because it gives realistic stress strain loops, while being simple. It should be noted that the proposed function is even and that because of the rotation, the rotated axes have no meaningful units. However, as shown later, the stress is not actually calculated in the transformed coordinate system, only in the initial system, and the coordinate transformation is nothing more than a mathematical trick to satisfy desired damping conditions. The shape of the function describing a half loop in the transformed coordinate system is shown in Figure 2.

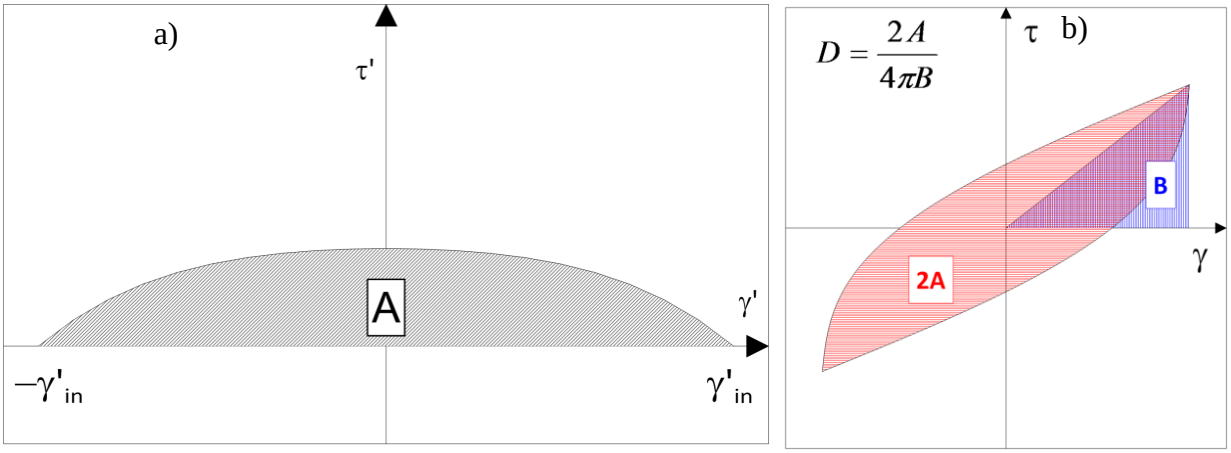

Figure 2. a) Half loop in the transformed coordinate system, and b) definition of damping

Figure 2(a) introduces the target reversal strain in the transformed system:

$$\gamma'_{in} = \frac{\gamma_R - \gamma_0}{cos\theta} \tag{7}$$

To derive the three coefficients *a*, *b*, and *c*, we define the three following conditions:

$$f(x) = 0 \; at \; x = \pm \gamma'_{in} \tag{8}$$

$$\int_{-\gamma'_{in}}^{\gamma'_{in}} f(x)dx = A = \gamma'_{in} D\pi(\tau_R - \tau_0)cos\theta \tag{9}$$

$$f''(x) \leq 0 \; for \; x \in -\gamma'_{in}..\gamma'_{in} \tag{10}$$

The Equation 8 ensures that the loop closes, and that the transformed stress is 0 at the target reversal point (see half loop on Figure 2(a)). Equation 9 makes sure that the area under the loop satisfies the damping curve. The area under the half loop is A. The damping ratio is defined by D=2A/(4πB). *B* is the area of the triangle shown on Figure 2(b) and is equal to:

$$B = \frac{(\tau_R - \tau_0) * (\gamma_R - \gamma_0)}{2} \tag{11}$$

Equation 9 is obtained by plugging Equation 7 in 11. The damping ratio D is linearly interpolated from the input damping curve with the strain axis being a logarithm scale, based on the equivalent shear strain level:

$$\gamma_{eq} = \frac{|\gamma_R - \gamma_L|}{2} \tag{12}$$

If the loading is symmetrical then γ_L =-γ_R, and the strain used to calculate D is simply $\gamma_{in_{max}}$. Equation 10 ensures that the curve is concave rendering a more realistic shape to the stress-strain curve. A bi-quadratic equation has maximum two inflection points where $f''(x) = 0$, that are symmetrical with respect to the y-axis. If we force the inflection points to be at $\pm\gamma'_{in}$ then the condition is automatically satisfied. Equations 8, 9 and 10 reduce to the following system of equations:

$$a\,\gamma'_{in}{}^{4} + b\,\gamma'_{in}{}^{2} + c = 0 \tag{13}$$

$$\frac{2}{5}a\,\gamma'_{in}{}^{4} + \frac{2}{3}b\,\gamma'_{in}{}^{2} + 2c = D\pi(\tau_R - \tau_0)cos\theta \tag{14}$$

$$12a\,\gamma'_{in}{}^{2} + 2b = 0 \tag{15}$$

This system of equations can easily be solved using matrices to obtain the coefficients *a*, *b*, and *c* that satisfy the three conditions. Combining Equations 4, 5, and 6, a relationship between strain and stress can be derived in the original coordinate system:

$$\tau = [(\gamma - \gamma_0)\cos\theta + (\tau - \tau_0)\sin\theta]\sin\theta + [a((\gamma - \gamma_0)\cos\theta + (\tau - \tau_0)\sin\theta)^4 + b((\gamma - \gamma_0)\cos\theta + (\tau - \tau_0)\sin\theta)^2 + c]\cos\theta + \tau_0 \tag{16}$$

In this equation everything is known except the stress τ. To solve this equation we use the Ridders' Method (Ridders 1979), an algorithm based on the false position method in which convergence is guaranteed as long as the two initial guesses lie on each side of the root. This is satisfied by using the stress at the previous time step and the target stress point as initial guesses. Convergence is ensured independently of the amplitude of the strain increment. Other methods converge more rapidly (e.g., Newton-Raphson), but are not always able to converge upon the desired root. Ridders' method cannot fail once the root is bracketed, and converges more quickly than the bisector method.

Asymmetrical Loading

The previous section describes the constitutive equations of the model and introduces the notion of target and previous reversal points, respectively (γ_R, τ_R) and (γ_L, τ_L). When the loading is symmetric, the previous point is the maximum reversal stress-strain point and the target point is the opposite of the maximum reversal stress-strain point. In this section we present how (γ_R, τ_R) and (γ_L, τ_L) are selected from a vector of possible values when the loading is asymmetrical. The vectors of stress and strain reversal points update in a similar fashion. For the sake of brevity we only present the procedure to update the strain vectors.

The model keeps track of the reversal points in vectors containing the possible values of the target and previous reversal points. When reversal occurs, the direction of the strain increment changes, and the previous reversal point becomes the target reversal point while the current reversal point becomes the previous reversal point γ_L. When the current strain is greater than the target reversal strain (γ_R), the target reversal strain becomes the next reversal point in the

direction of loading. The previous reversal point is also updated, and taken at the next reversal point in the opposite direction of loading. When the points are updated without change of direction of loading, the previous values are deleted from the vectors of possible values. Figure 3 presents an example of how the previous and target reversal points are selected.

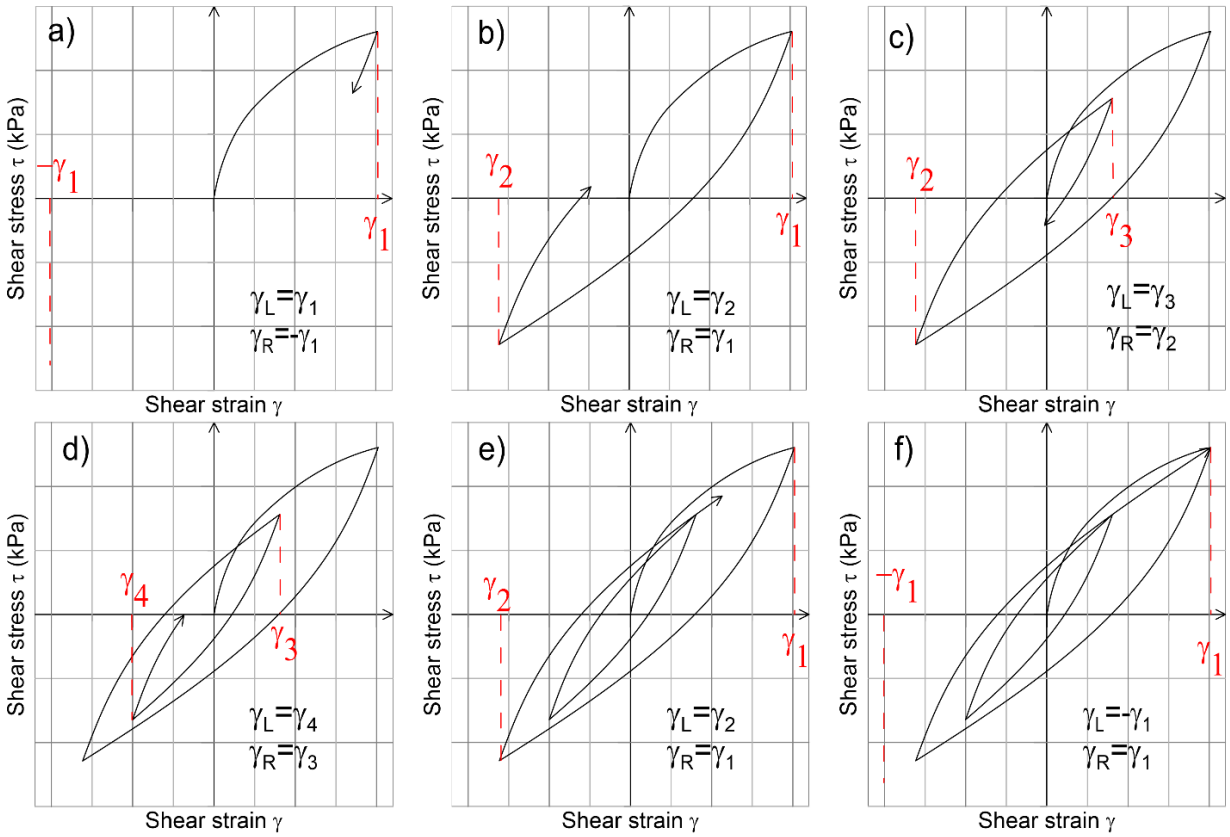

Figure 3. Evolution of the reversal strain vectors

Performance of the Model

Influence of Strain Increment Amplitude

As mentioned earlier, the model is able to predict the correct stress for any strain increment. Figure 4 presents the prediction of the model for a sample of clay subject to sinusoidal loading at different strain levels. The target damping and modulus reduction curves are calculated from Darendeli for a soft clay with the following characteristics: PI=40, σ'_v=47.5 kPa, γ=15 kN, V_s=80 m/s, OCR=1.15 K_0=0.5. The modulus reduction is also modified following the procedure of Yee et al. (2013), to match a target undrained strength (S_u) of 17 kPa. The transition strain was set to 0.03%. The target curves are presented on Figure 5. Figure 4 shows that predictions for a cycle defined by 20 points lie exactly on the curves described by 200 points, at every strain levels. This is because the stress is calculated directly as a function of the current strain and does not depend on the amplitude of the strain increment. Figure 4(a) also illustrates how hysteretic damping is introduced at low shear strain level where the soil does not exhibit any modulus reduction.

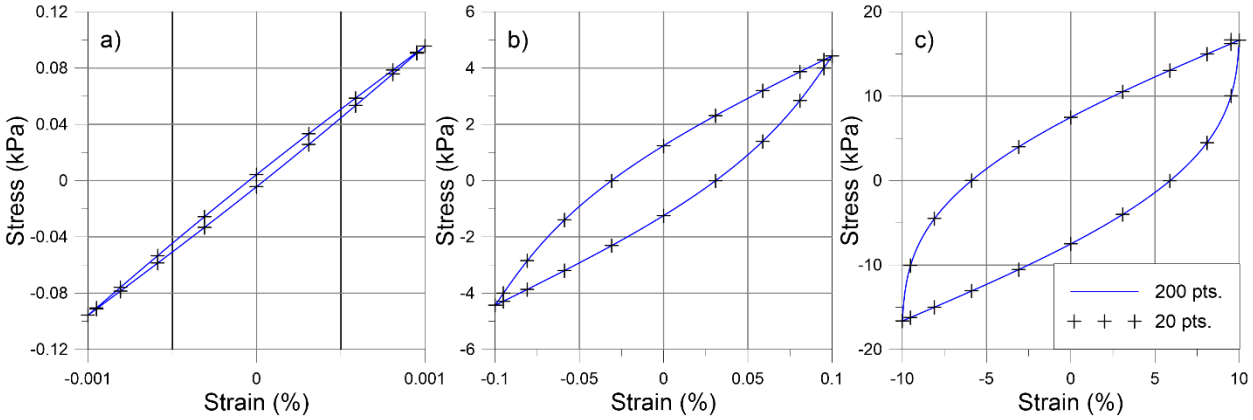

Figure 4. Comparison of the predictions of the model for cycles defined by 20 and 200 points at strain levels of (a) 0.001%, (b) 0.1%, (c) 10%.

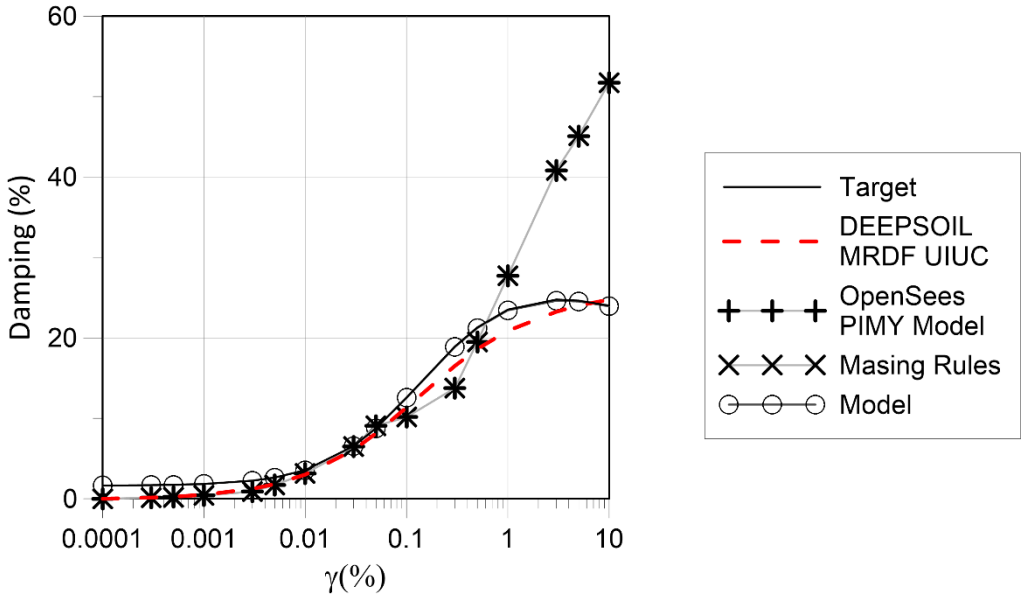

Figure 5. Hysteretic damping curves predictions of different models for a clay PI=40 σ'_v=47.5 kPa, γ=15 kN, V_s=80 m/s, OCR=1.15 K_0=0.5.

Comparison with Existing Models

Figure 5 is a comparison between our model and different existing model: MRDF UIUC used in Deepsoil (Phillips and Hashash 2009), the PressureIndepMultiYield (PIMY) Model in OpenSees (Elgamal et al., 2003), and Masing's rules. The target curves were the same as described previously.

Neither the PIMY nor MRDF UIUC model capture small-strain hysteretic damping. Small strain damping is typically modeled using Rayleigh damping, which is either frequency-dependent (i.e., two-point Rayleigh damping in OpenSees) or computationally demanding (frequency-independent damping in DeepSoil).This results in a pretty close match of the damping curve. Our

coordinate transformation model perfectly matches the damping curve, at all strain levels. This avoids the need for Rayleigh damping, and also avoids over-damping at high strain that is associated with Masing's rules.

Conclusions

A new unloading and reloading rule uses a coordinate transformation approach to precisely match a desired modulus reduction and damping curve, regardless of the amplitude of the strain increment. The model captures small-strain hysteretic damping, thereby eliminating the need for Rayleigh damping, and it does not over-damp at high strain, which is a well-known problem associated with Masing's rules. The model is well suited for 1D site response analysis, though it is not yet implemented in a site response code. Furthermore, a multi-axial generalization could permit the model to be used in 2D or 3D numerical simulations. Implementation and extension of the model is reserved for future publications.

Acknowledgments

This research was funded by the National Science Foundation under grant No. CMMI 1208170. Any opinions, findings, and conclusions or recommendations expressed in this material are those of the authors and do not necessarily reflect the views of the National Science Foundation. The authors would like to thank Professor Jonathan Stewart from UCLA for his input on the model.

References

Darendeli M. B., *Development of a New Family of Normalized Modulus Reduction and Material Damping Curve.* Ph.D. Dissertation, University of Texas at Austin, Austin 2001.

Elgamal A., Yang Z., Parra E., Ragheb A., Modeling of cyclic mobility in saturated cohesionless soils. *International Journal of Plasticity*, 2003, **19**: 883-905.

Hashash Y. M. A., Phillips C., and Groholski D. R., Recent advances in non-linear site response analysis. *Fifth International Conference on Recent Advances in Geotechnical Earthquake Engineering and Soil Dynamics*, San Diego 2010.

Phillips C., and Hashash Y. M. A., Damping formulation for nonlinear 1D site response analyses. *Soil Dynamics and Earthquake Engineering*, 2009, **29** (7): 1143-1158.

Rayleigh, J.W.S and Lindsay R.B., *The Theory of Sound*, Dover Publications, New York, 1945

Ridders C. J. F., A new algorithm for computing a single root of a real continuous function. *IEEE Transactions on circuits and systems*, 1979, **26**: 979-980.

Wang Z.L., Dafalias Y.F., Shen C.K., Bounding surface hypoplasticity model for sand. *Journal of Engineering Mechanics*, 1990, ASCE, **116** (5): 983-1001

Yee E., Stewart J.P., Tokimatsu K., Elastic and large-strain nonlinear seismic site response from analysis of vertical array recordings, *Journal of Geotechnical and Geoenvironmental Engineering*, 2013, **139** (10): 1789-1801.